APPLICATION OF SHOCK CAPTURING AND CHARACTERISTICS METHODS TO SHUTTLE FLOW FIELDS

By P. Kutler, J. V. Rakich, and G. G. Mateer

NASA Ames Research Center
Moffett Field, California

INTRODUCTION

The ultimate objective of the work described herein is to calculate real gas flows, including rate chemistry, around the space shuttle vehicle. This would permit the prediction of the heating and heat-shield erosion for actual flight conditions, something that no present wind tunnel can do completely. A limiting factor in the simulation of real gas flows is the speed of present computers. Fortunately, advanced computers such as STAR and ILLIAC will soon be available and they have the potential for such computations. In fact, ILLIAC is scheduled for installation here at Ames Research Center this summer. With this goal in mind, and in anticipation of ILLIAC, advanced techniques are now being developed which can exploit the unique capabilities of ILLIAC.

Methods for computing complicated inviscid supersonic flows in three space dimensions have been under development at Ames Research Center for several years. Two fundamentally different approaches are being used and are discussed in this paper. The first and oldest is based on the method of characteristics[1] (referred to as MOC in the following discussion). The particular technique used in this program is referred to in the literature as a "reference-plane" or "semicharacteristic" method, since finite difference relations are used to treat certain cross derivatives. The second and newest method[2] utilizes the gas-dynamic equations in conservation-law form and automatically allows for the existence and formation of shock waves without special application of the Rankine-Hugoniot conditions (referred to as a shock capturing technique, or SCT in the following discussion). An explicit second or third order noncentered, finite-difference scheme is used to solve the governing equations.

This paper will show some recent results obtained with these methods for an early orbiter shape proposed by the North American Rockwell Corporation and also for the more recent 040A configuration suggested by NASA-MSC. Results obtained with the SCT code demonstrate its three-dimensional, multiple shock capturing capability while results obtained with the MOC code demonstrate the calculation of equilibrium real gas flows and the determination of flow variables required for a heating analysis.

SHOCK SHAPES FOR SIMULATED NARC SHUTTLE ORBITER

(Figure 1)

Initial efforts to calculate the flow field for the NARC space shuttle orbiter included a pointed nose to simplify determination of the initial conditions. For this case, the SCT code generated its own starting solution, however, subsequent calculations, which utilized blunted noses, relied on the use of the inverse blunt body method[3] and the MOC code[1] to generate the required starting data. A typical body cross section for the NARC orbiter was approximated by two ellipses whose semi-major and minor axes varied as cubic polynomials between a discrete number of longitudinal stations (see ref. 4). Simulation of the wing on the NARC orbiter was included by varying the semi-major axes of the ellipses according to the wing planform. The canopy for this example was excluded, but has been included in subsequent calculations.

The shock pattern predicted for this configuration by the SCT code is shown in Figure 1 for both the planform and profile views. At an x/L of .6, a shock appears off the leading edge of the wing as a result of the compressive turning of the flow in that vicinity. As the calculations proceed downstream, the shock wave starts to move further from the wing. This is a result of the thick wing approximated by the top ellipse. The wing leading-edge shock eventually intersects the bow shock at an x/L of about .78 and extends beyond it at stations further downstream of this point. The main point of this calculation was to demonstrate that the SCT code is capable of predicting the formation of secondary shock waves and, also, shock-shock intersections. For this calculation the computational plane was discretized into 30 points in the radial direction and 19 points in the meridional direction The integration procedure required 1×10^{-4} minutes per point and the entire calculation consumed approximately 19 minutes on an IBM 360/67 with interactive graphics.

As indicated in the figure, the MOC code gave virtually identical shock shapes up to about x/L = 0.6. The MOC code had difficulty in proceeding beyond that point because of the secondary shock.

SHOCK SHAPES FOR SIMULATED NARC SHUTTLE ORBITER

M = 5 α = 5°

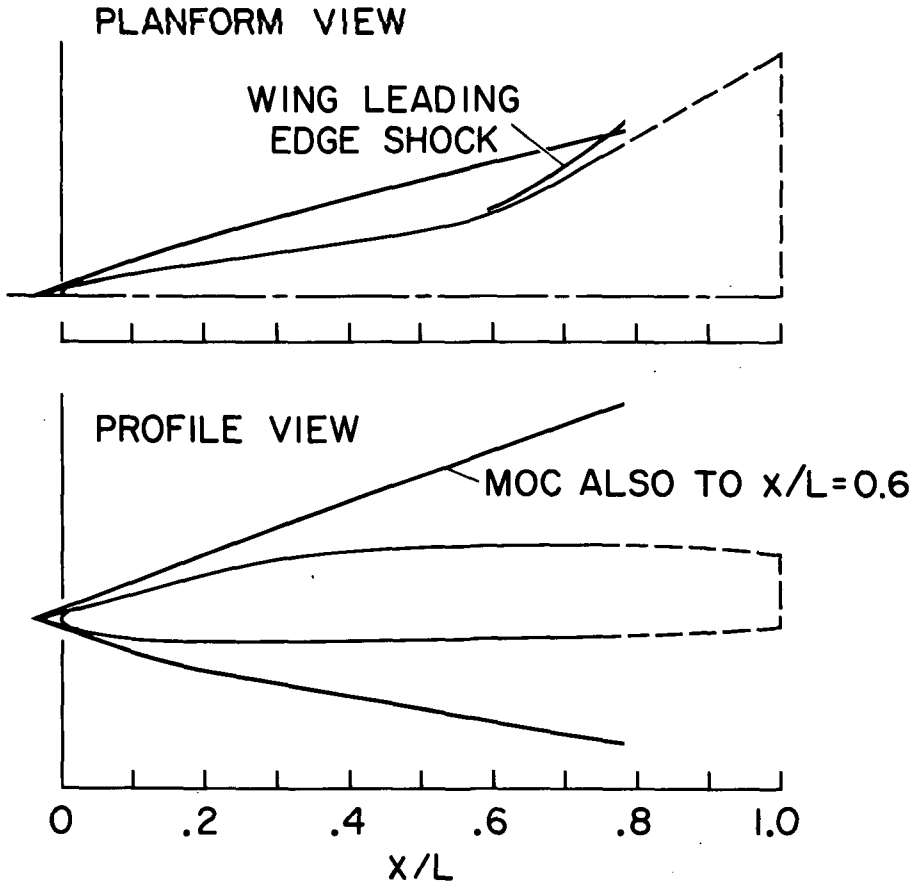

Figure 1

CROSS SECTIONAL SHOCK SHAPES FOR NARC SHUTTLE ORBITER

(Figure 2)

The cross sectional shock shapes and simulated body shapes are shown in Figure 2 for three longitudinal stations. At an x/L of .66 there is a clearly defined leading edge shock which just stands off the body. Further downstream at an x/L of .785 the leading edge shock intersects and extends beyond the main bow shock. This complicated three-dimensional shock pattern presented no problems for the SCT code. In the future the analytical description of the body will be improved, especially in the vicinity of the wing leading edge. It is believed that such changes will have only a minor effect on the windward portion of the flow, but a noticeable effect on the standoff distance of the wing leading edge shock wave.

The limiting factor in these calculations is the computer and not the method. More mesh points are needed in the vicinity of the wing leading edge to properly resolve the rapid variation of the flow there. Utilization of a finer mesh will become possible with advanced computers such as ILLIAC.

In principle, complicated shock intersections, such as shown in Figure 2 can be treated by the method of characteristics also. However, the programming for intersecting shocks is extremely difficult. With the SCT code, the programming is simple and the calculations routine.

CROSS SECTIONAL SHOCK SHAPES FOR NARC SHUTTLE ORBITER

M = 5 α = 5°

—— SIMULATED CONFIGURATION

— — — ACTUAL CONFIGURATION

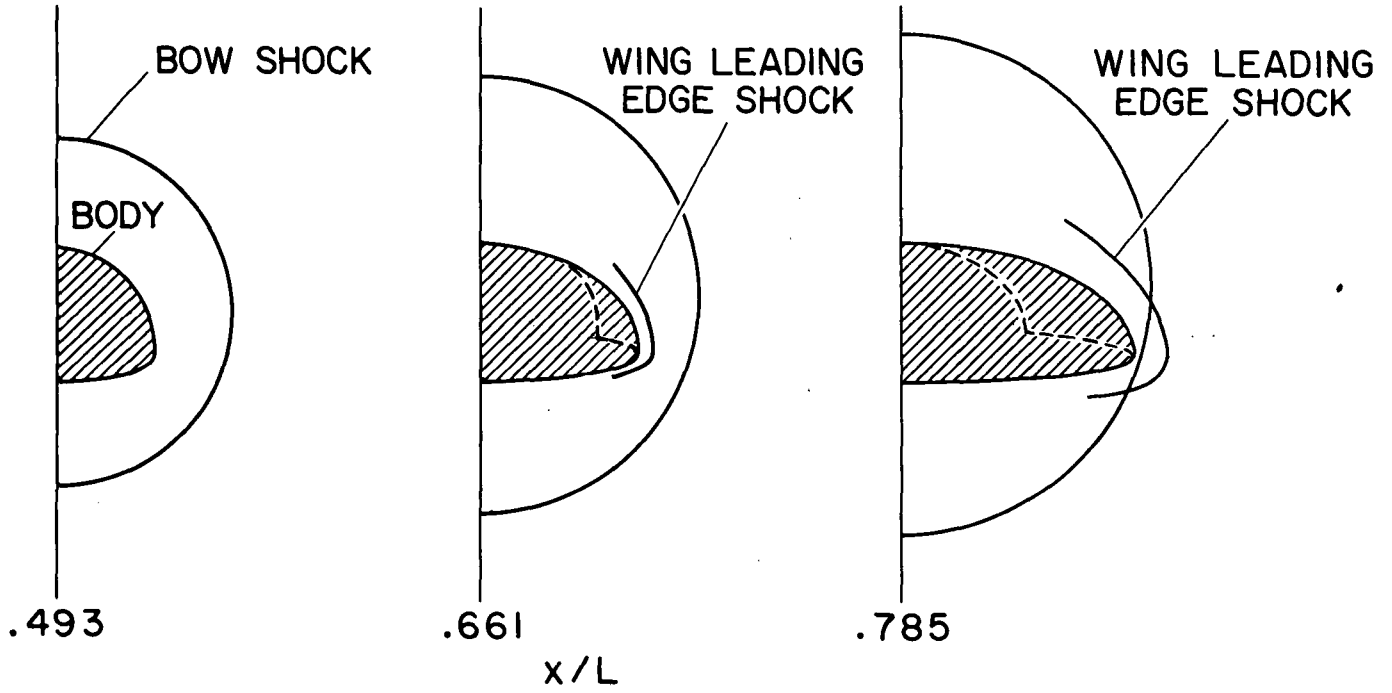

Figure 2

LONGITUDINAL SURFACE PRESSURE DISTRIBUTION FOR NARC SHUTTLE ORBITER

(Figure 3)

The variation of surface pressure coefficient with longitudinal distance for the 0°, 90°, and 180° meridians is shown in Figure 3. The constant pressure coefficient near the nose is a result of the cone solution. The 90° meridian contains the simulated wing leading edge, and as the flow is turned due to the presence of the wing the pressure rises rapidly. It begins to decrease as the leading edge reaches its final swept position and the secondary shock moves away from the surface. Of course, a sharp peak in heating is expected to accompany the pressure rise.

The irregularities in the pressure distribution arise from the body description which matched slopes but allowed curvatures to be discontinuous. Similar pressure variations were obtained from the MOC code and agreement is excellent; numerous comparisons of the two methods are given in reference 4.

LONGITUDINAL SURFACE PRESSURE DISTRIBUTION FOR NARC SHUTTLE ORBITER

M = 5 α = 5°

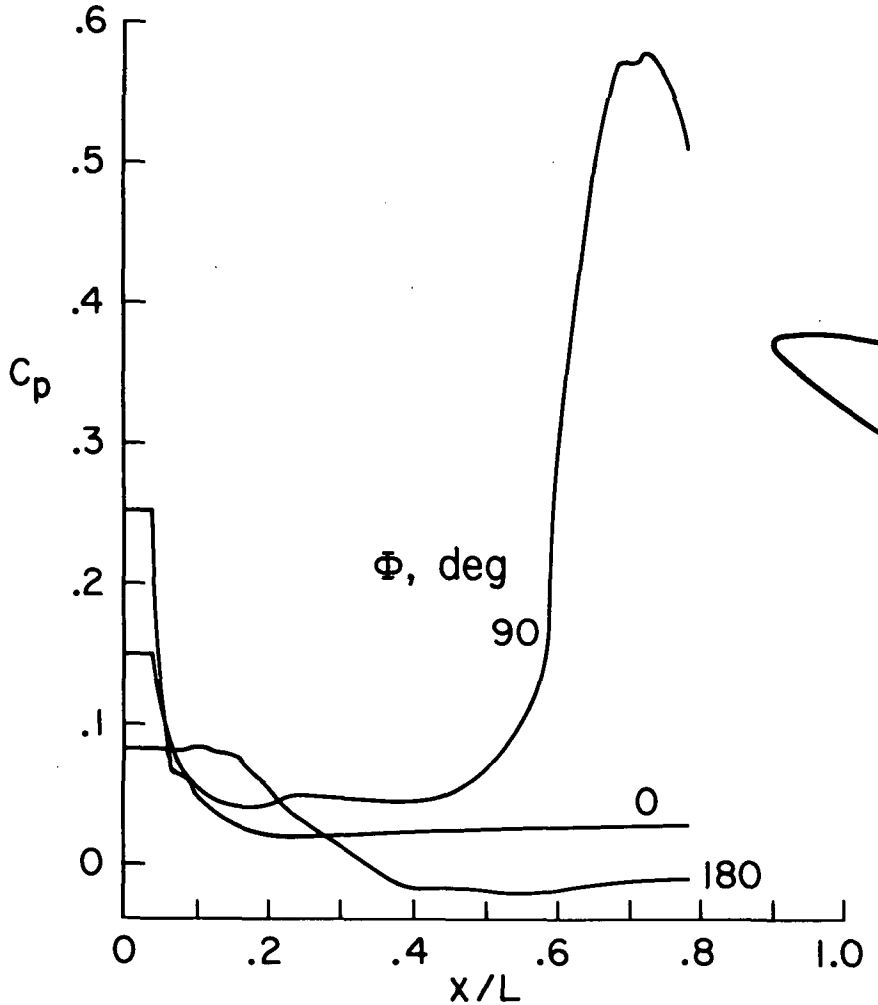

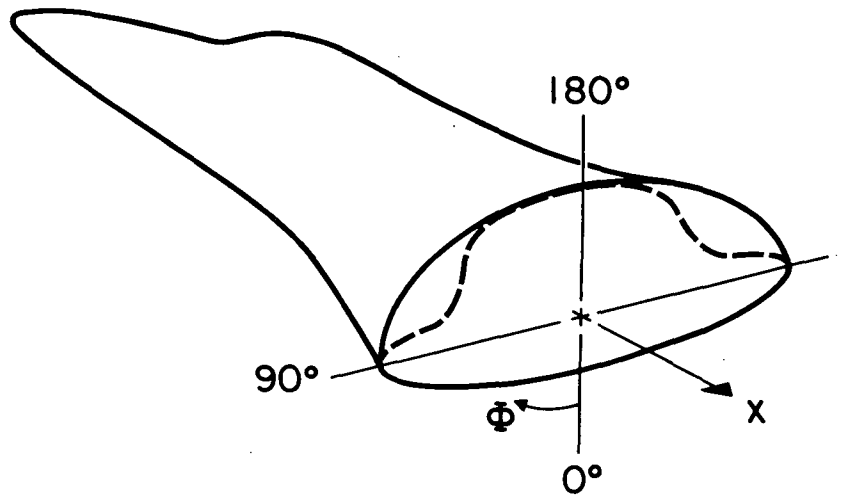

Figure 3

SHOCK LOCATION FOR BLUNTED SHUTTLE ORBITER

(Figure 4)

Figure 4 shows the shock shape for a blunt nosed version of the same body. Also, a more realistic approximation for the canopy has been made here. The angle of attack is 15.3° and M = 7.4. Comparison is made with experiment (shadowgraph) obtained by J.W. Cleary[5] in the Ames 3.5-foot Hypersonic Wind Tunnel. Agreement between theory and experiment is excellent for the bow wave. The small differences for the canopy wave are believed due to an inexact modeling of the canopy shape.

The good agreement with experiment provides confidence in the shock capturing method. In addition, the method is able to resolve a weak recompression shock behind the canopy shock, although the recompression shock was too weak to show in the shadowgraph.

Results of the MOC code are in reasonable agreement with SCT code (and experiment) for the bow shock. However, the MOC code does not resolve the canopy shock very well.

SHOCK LOCATION FOR BLUNTED SHUTTLE ORBITER AT ANGLE OF ATTACK

M = 7.4 α = 15.3°

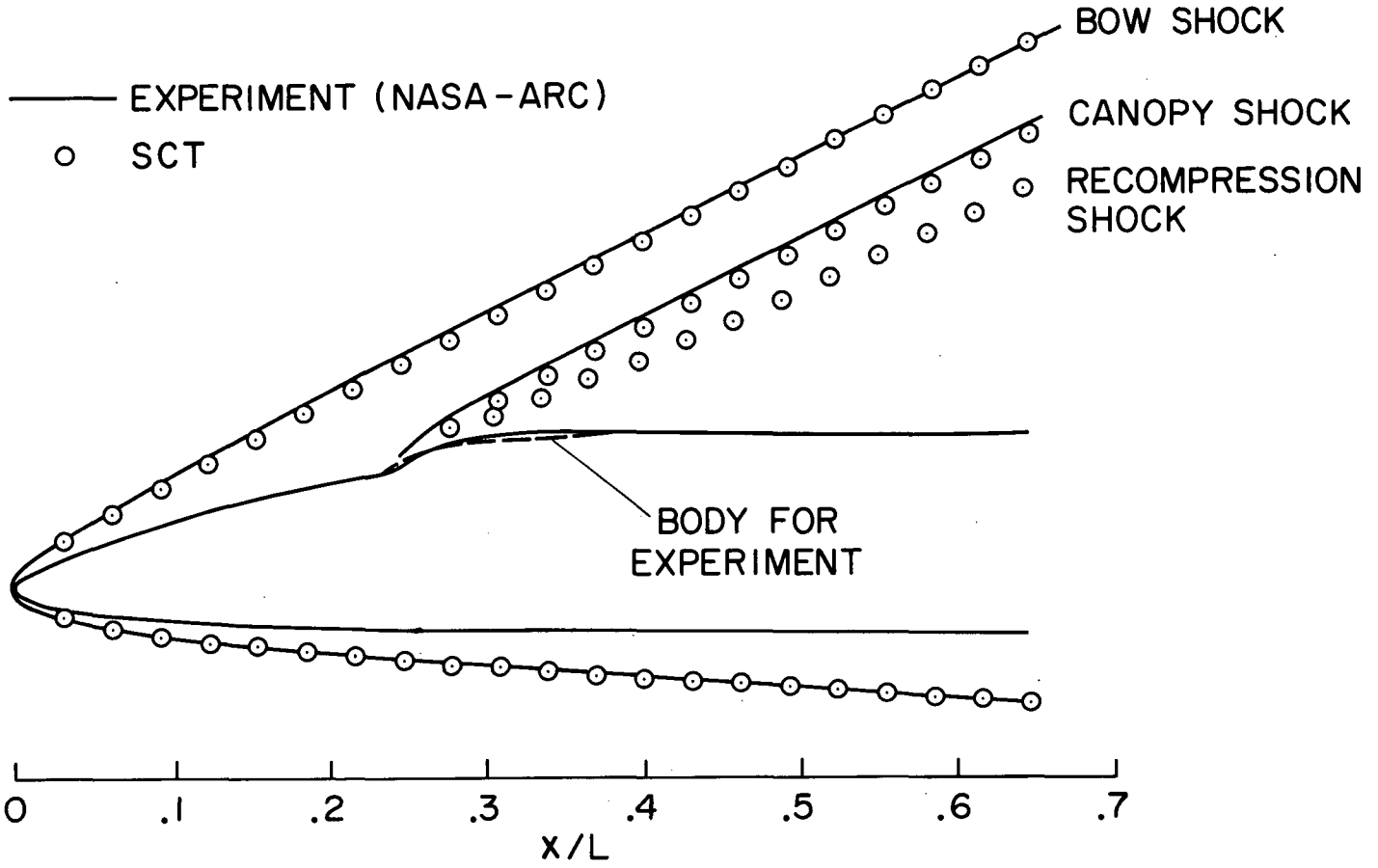

Figure 4

SHOCK SHAPE FOR NARC SHUTTLE ORBITER

(Figure 5)

The next set of figures shows the effect of equilibrium gas properties on the flow over the North American Rockwell orbiter. The calculations were performed with the MOC code[1] and using the Ames RGAS tables.[3] Equilibrium calculations correspond to a flight velocity of 7.3 km/sec (24,000 fps or M = 26.3) and with ambient conditions corresponding to 76 km (250,000 ft) altitude. Comparisons are made with perfect gas calculations at M = 7.4, for which experimental data are available. It should be noted that there are no ground test facilities that can simulate these flight conditions.

Figure 5 shows the bow shock shapes on the vertical plane of symmetry. The equilibrium shock standoff distance is about half the perfect gas value. Part of the difference is due to the different Mach numbers, but it is believed that most of the difference is due to dissociation of molecular oxygen. The perfect gas results are in reasonably good agreement with the experimental shock shape shown in Figure 4. Thus, while these experimental results are useful for checking the numerical calculations, experimental shock shapes are not easily extrapolated to flight conditions. This has a bearing on the design of a thermal protection system for areas where the bow shock may intersect the wing or control surfaces.

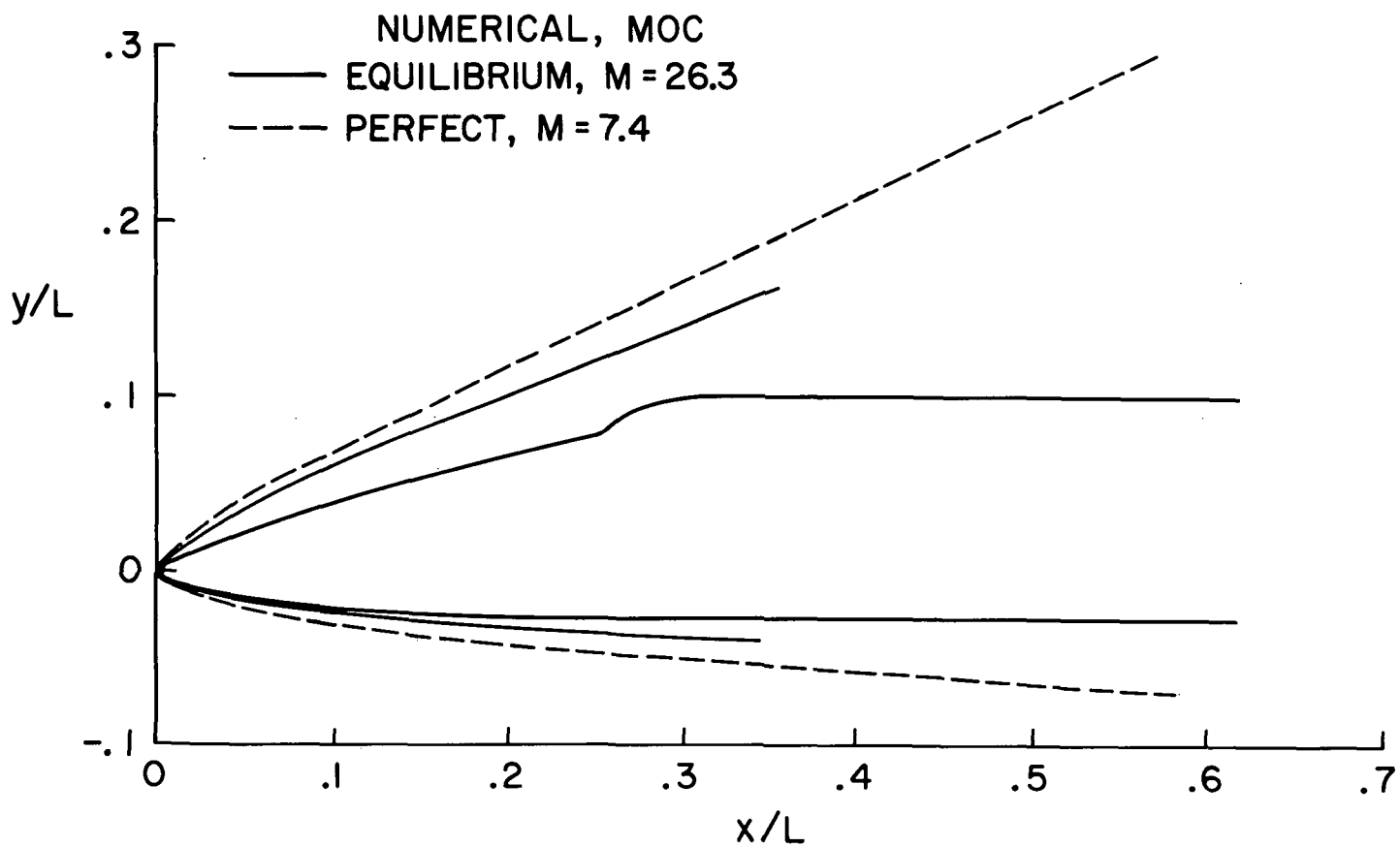
SHOCK SHAPE FOR NARC SHUTTLE ORBITER
EQUILIBRIUM AND PERFECT GAS
α = 15.3°
NUMERICAL, MOC
EQUILIBRIUM, M = 26.3
PERFECT, M = 7.4
y/L
.3
.2
.1
0
-.1
0
.1
.2
.3
.4
.5
.6
.7
x/L

Figure 5

SURFACE PRESSURES FOR NARC SHUTTLE ORBITER

(Figure 6)

A comparison of surface pressures is shown in figure 6. In this case there is only a small difference between the perfect and equilibrium real gas results. The effect of the different Mach numbers is accounted for in the pressure coefficient. Experimental pressures obtained by C. C. Pappas in the Ames 3.5-foot hypersonic wind tunnel are also shown. The small differences between theory and experiment in the vicinity of the nose are attributed to differences between the model and theoretical body shapes.

These calculations with the MOC code employed from 11 to 21 points between the body and shock on each of 19 meridional planes. The real gas calculations take about 60% longer than for the same perfect gas case. For the perfect gas, the unit computation time is about 4×10^{-4} minutes per point on an IBM 360/67 computer; total times to $x/L = .34$ are about 80 min. for a perfect gas and 120 min. for a real gas.

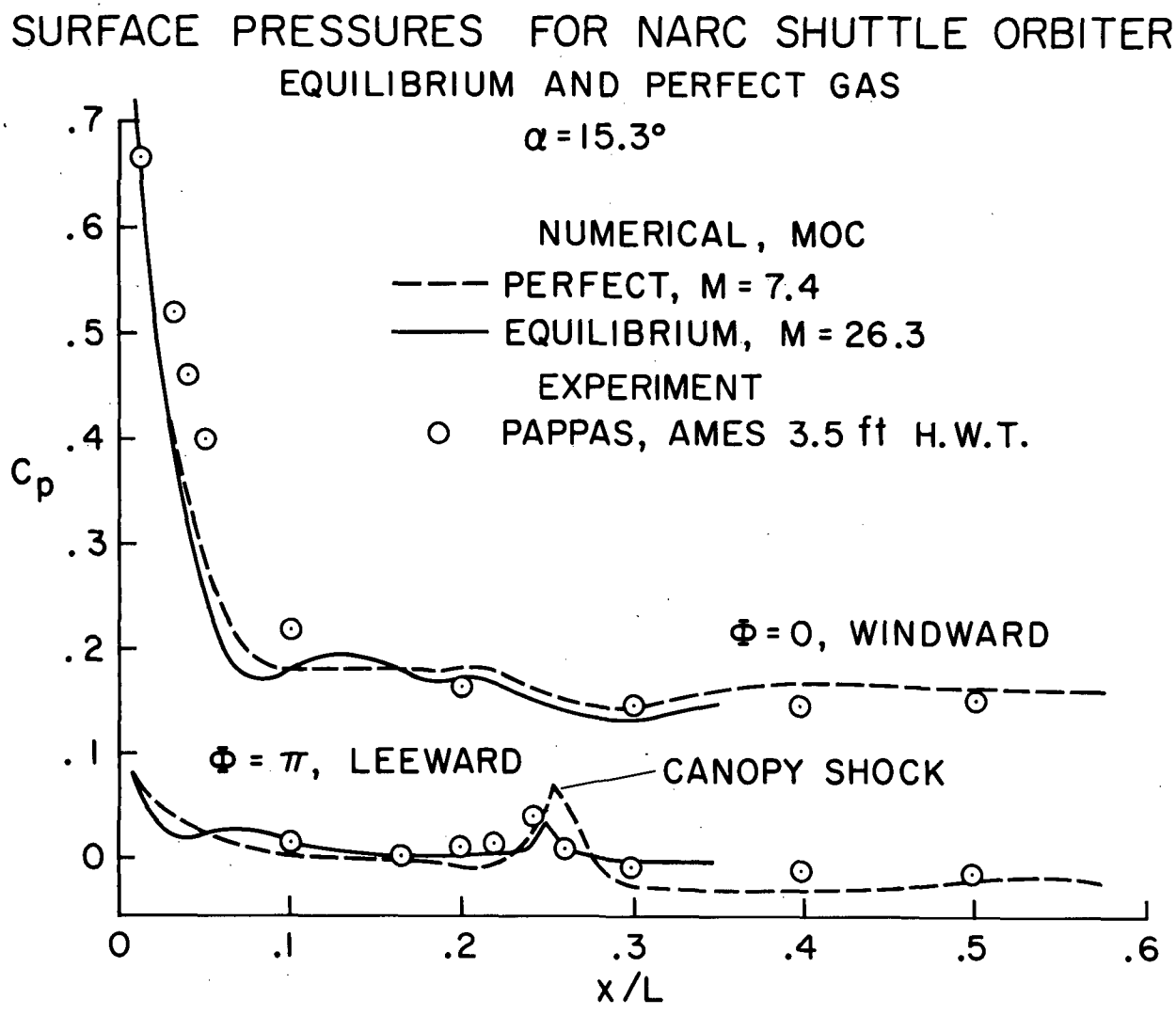
SURFACE PRESSURES FOR NARC SHUTTLE ORBITER
EQUILIBRIUM AND PERFECT GAS
α = 15.3°
NUMERICAL, MOC
PERFECT, M = 7.4
EQUILIBRIUM, M = 26.3
EXPERIMENT
PAPPAS, AMES 3.5 ft H.W.T.
Cp
.7
.6
.5
.4
.3
.2
.1
0
Φ = 0, WINDWARD
Φ = π, LEEWARD
CANOPY SHOCK
0
.1
.2
.3
.4
.5
.6
x/L

Figure 6

SURFACE ENTHALPY AND DENSITY FOR NARC SHUTTLE ORBITER

(Figure 7)

Figure 7 shows two local flow variables, enthalpy, H, and density, ρ, that cannot readily be simulated in ground based tests. These variables, as seen in the figure, are very different for equilibrium and perfect gas flows. The enthalpy ratio is related to velocities by the energy equation as follows:

$$H/H_T = 1 - \frac{V^2}{2H_T}$$

Together with the pressure and viscosity, these quantities affect the aerodynamic heating in a complex way which can only be predicted with a detailed boundary-layer calculation. The present numerical methods provide all of the information needed for such a boundary-layer solution and heat-transfer analysis.

SURFACE ENTHALPY AND DENSITY FOR NARC SHUTTLE ORBITER

EQUILIBRIUM AND PERFECT GAS

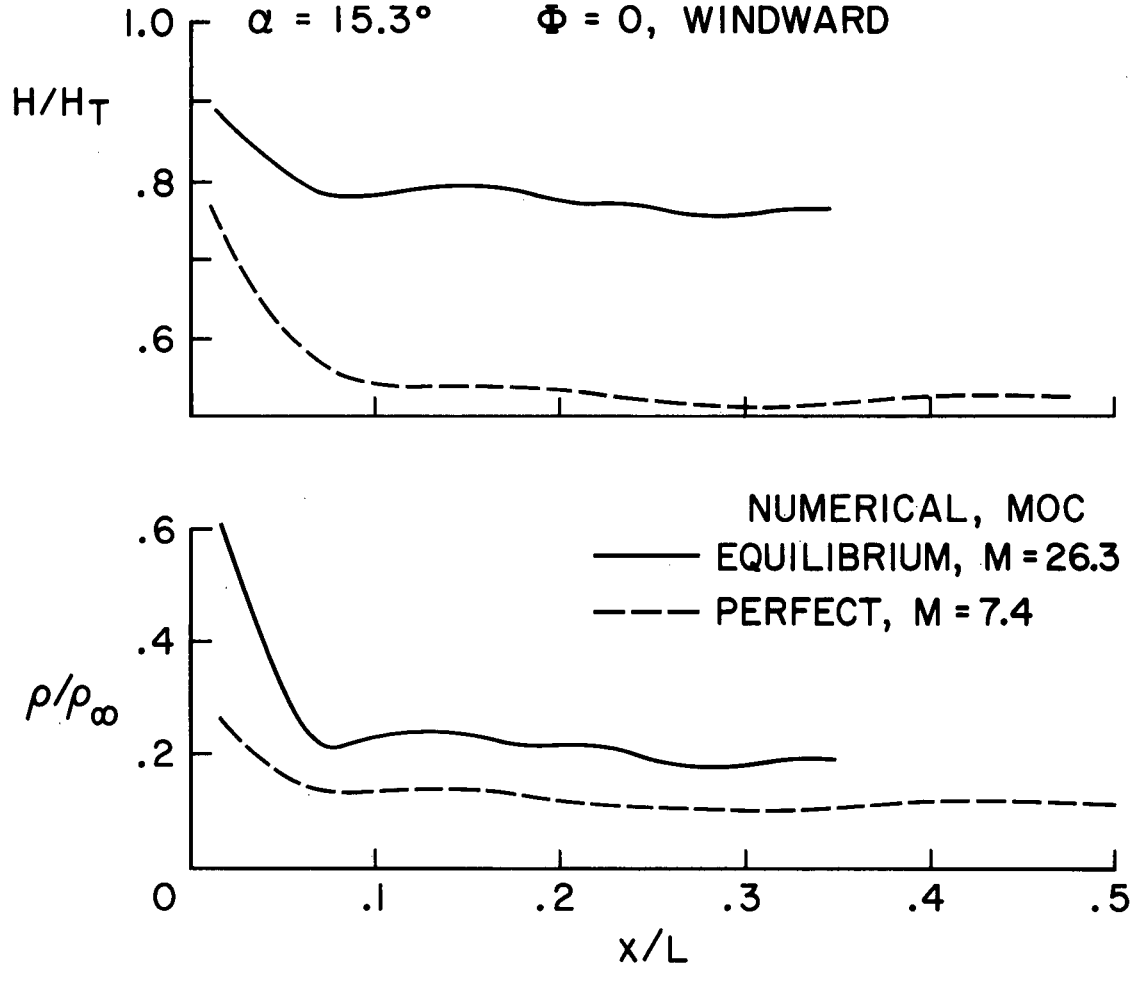

Figure 7

STREAMLINE METRIC FOR NARC SHUTTLE ORBITER

(Figure 8)

For three-dimensional flows such as that over the space shuttle, the boundary layer and heating analysis is complicated by the curved path of the streamlines. Most heating analyses require the metric coefficients for the curvilinear streamline coordinates, which are not known a-priori but can be determined from the inviscid flow field. The metric, h, which determines the distance between streamlines (see sketch in Fig. 8) is most important and is automatically calculated in the present MOC program.

As an example, figure 8 shows the variation of h on the windward plane of symmetry. For this special case the equation governing the change in h with axial distance x has two parts:

$$\frac{r}{h}\left(\frac{\partial h}{\partial x}\right)_{\Phi=0} = \left(\frac{\partial r}{\partial x}\right) + \frac{1}{u}\left(\frac{\partial w}{\partial \Phi}\right) \qquad (1)$$

The first term in Eq. (1) is due to the local body slope, and the second term is due to the crossflow velocity gradient. When the velocity gradient vanishes, then h is the local cylindrical radius, r. When $\partial r/\partial x = 0$, as on a large part of the shuttle, h depends on $\partial w/\partial \Phi$ where w is the cylindrical crossflow velocity. Therefore the crossflow velocity gradient causes h to increase initially as the streamlines are spreading out. The curve flattens out at about $x/L = .35$ due to the adverse crossflow pressure gradient which starts to develop there, and the streamline spreading diminishes.

STREAMLINE METRIC FOR NARC SHUTTLE ORBITER

PERFECT GAS

$M = 7.4 \qquad \alpha = 15.3° \qquad \Phi = 0$, WINDWARD

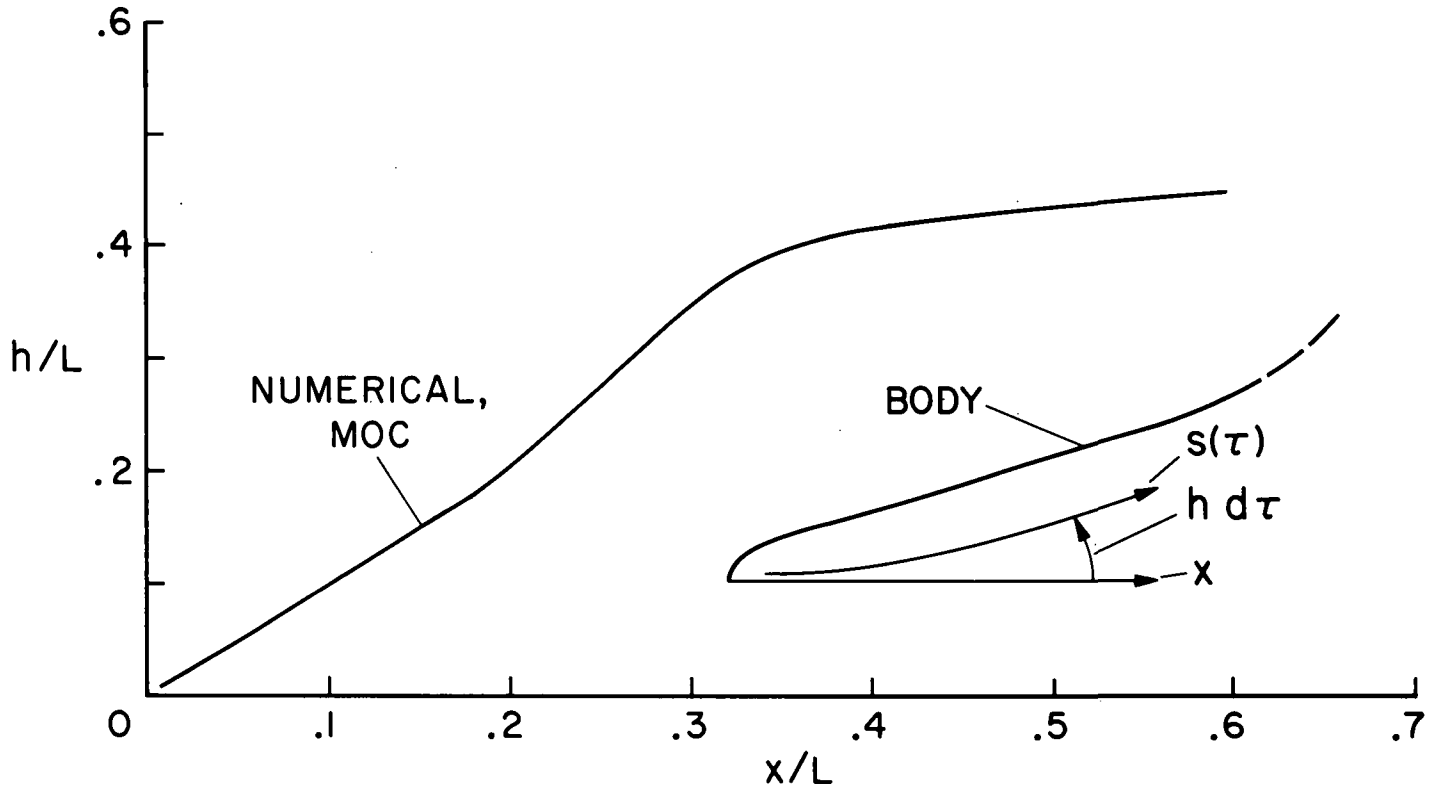

Figure 8

HEAT TRANSFER RATE FOR NARC SHUTTLE ORBITER

(Figure 9)

The axisymmetric or 2-D analog makes use of the fact that for small crossflow the 2-D boundary-layer equations have the same form as for 3-D flow, provided r is replaced by the metric h. Figure 9 shows the heating rate for the windward plane of asymmetry of the NARC shuttle orbiter, normalized by the stagnation heating to a sphere of 0.305 m (1-ft) radius. The metric coefficient from figure 8 was used with the boundary-layer program[6] developed by J. Marvin at NASA-Ames. These numerical predictions agree reasonably well with the data of Lockman and De Rose taken in the Ames 3.5-foot hypersonic wind tunnel.[7]

Also shown in Figure 9 is the predicted heat transfer to a flat plate (h=constant) for the same edge conditions. This comparison of the flat plate and actual heating rates illustrates the importance of knowing the correct streamline metric. The procedure for obtaining the metric and heating is similar to that described by Hamilton and DeJarnette[8]; the main difference is that the present method utilizes exact numerical flow field and boundary layer methods.

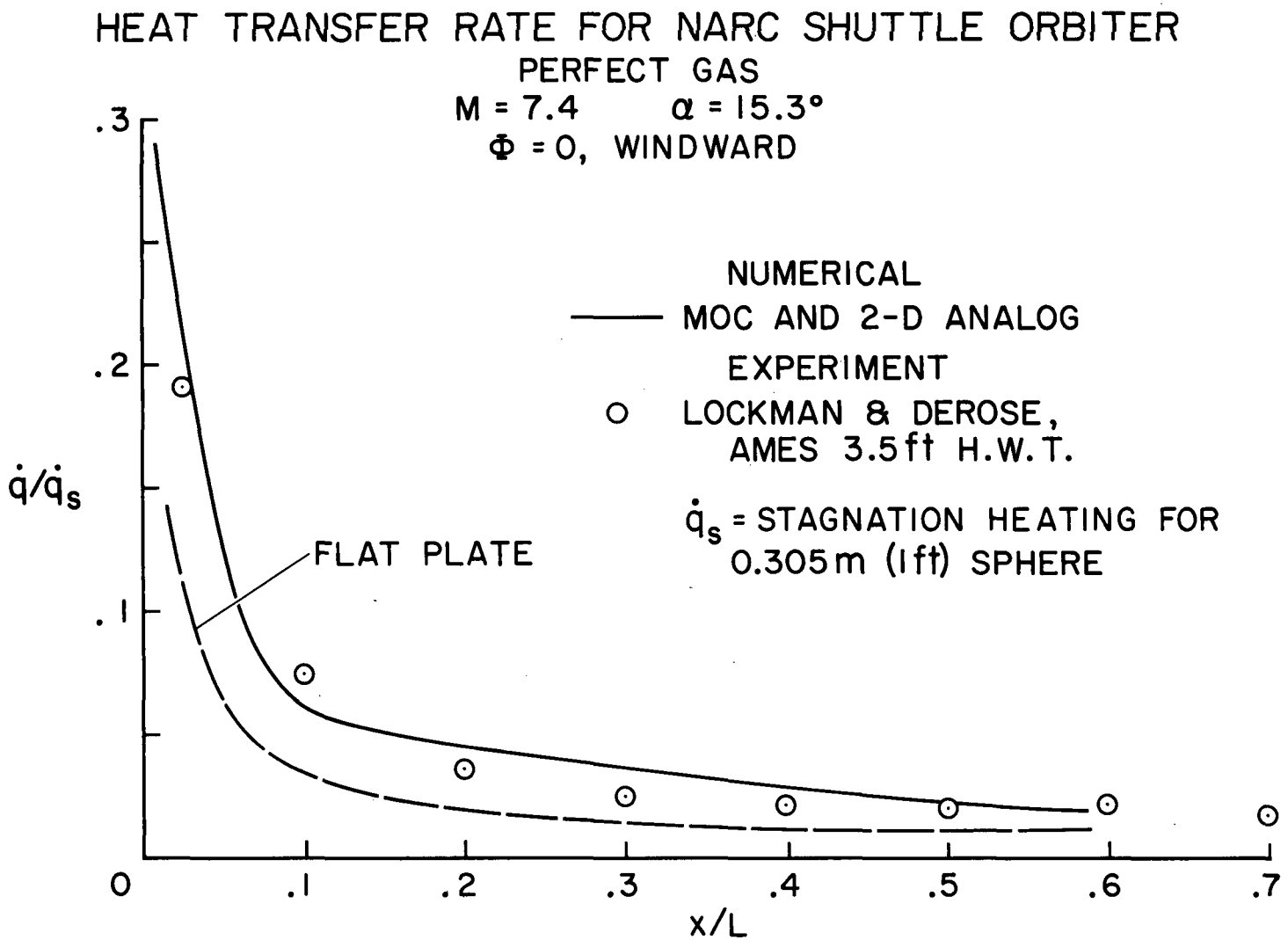
HEAT TRANSFER RATE FOR NARC SHUTTLE ORBITER
PERFECT GAS
M = 7.4 α = 15.3°
Φ = 0, WINDWARD
NUMERICAL
MOC AND 2-D ANALOG
EXPERIMENT
LOCKMAN & DEROSE, AMES 3.5ft H.W.T.
$\dot{q}_s$ = STAGNATION HEATING FOR 0.305m (1ft) SPHERE
FLAT PLATE
$\dot{q}/\dot{q}_s$
.3
.2
.1
0
.1
.2
.3
.4
.5
.6
.7
x/L

Figure 9

PROFILE AND PLANFORM SHOCK SHAPES FOR MSC 040A

(Figure 10)

In an attempt to determine the intersection of the bow shock with the wing of NASA's MSC 040A shuttle orbiter, the shock capturing technique[2] was used after obtaining a starting solution from an inverse blunt body code. For this calculation the wing and canopy were left off and a typical body cross section was simulated by two ellipses whose semi-major and semi-minor axes varied as cubic polynomials with longitudinal distance. The shock shape for the fuselage only configuration in Mach 7.4 flow at 15.3° angle of attack is shown in Figure 10 for both the planform and profile views. The shock location plotted in the planform view is the picture that an experimental shadowgraph would depict. Also shown is the intersection between the bow shock and the wing, which occurs well inside the projected shock trace because the body is at angle of attack. This is illustrated in the cross sectional shock shapes shown later.

SHOCK SHAPES FOR MSC 040A SHUTTLE ORBITER FUSELAGE ONLY

$M = 7.4 \qquad \alpha = 15.3°$

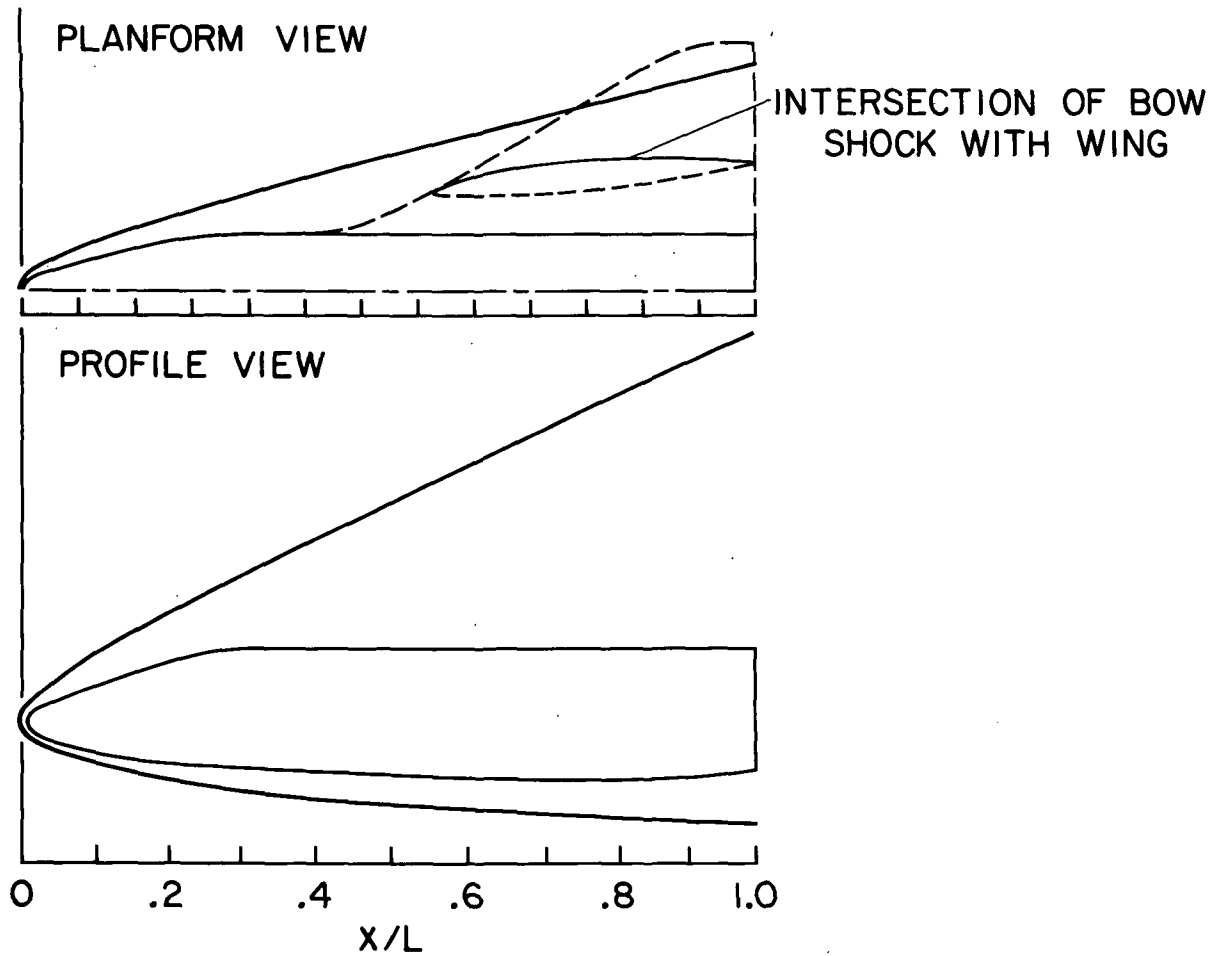

Figure 10

LONGITUDINAL SURFACE PRESSURE DISTRIBUTION FOR MSC 040A

(Figure 11)

The longitudinal variation of the surface pressure coefficient at three meridional locations of the MSC 040A fuselage is shown in Figure 11. Data is plotted beginning at the junction of the spherical nose and the three-dimensional afterbody. Due to numerical difficulties at the surface in the leeward plane the calculation was terminated at an x/L of .65. In approximating the 040A fuselage analytically by the present procedure, no constraint was place on the continuity of the second derivative (curvatures) of the body shape. This, therefore, can result in an unusual behavior of the solution at the matching points of the cubic polynomials. For the 040A the number of matching points was largest near the nose, in an attempt to accurately define it, and this resulted in the peculiar variations (plateaus) of the surface pressure distribution in that region. For this particular calculation the grid size consisted of 30 points in the radial direction and 19 points in the meridional direction. The large number of points was sufficient to clearly define the entropy layer at the surface. These results were obtained using a second-order noncentered, finite difference scheme. To calculate 65 percent of the body in 897 longitudinal steps required 54 minutes on an IBM 360/67 linked with an IBM 2250 cathode ray display tube.

LONGITUDINAL SURFACE PRESSURE DISTRIBUTION FOR MSC 040 A SHUTTLE ORBITER

FUSELAGE ONLY

M = 7.4 α = 15.3°

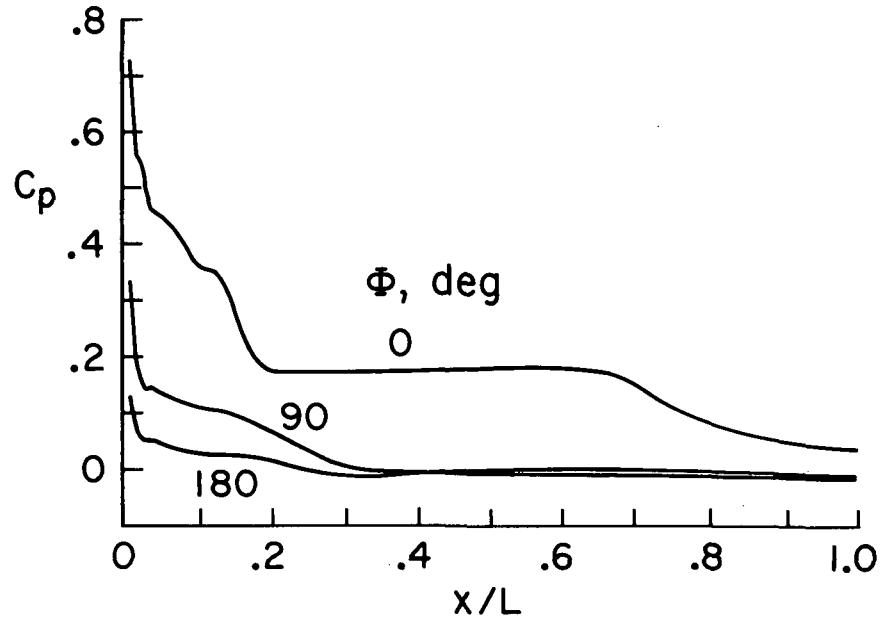

Figure 11

CROSS SECTIONAL SHOCK SHAPES AT VARIOUS LONGITUDINAL STATIONS FOR MSC 040A

(Figure 12)

The cross-sectional shock shapes of various longitudinal stations of the MSC 040A fuselage only configuration are shown in Figure 12. Also shown is a comparison of the actual body cross section with the simulated cross section. It can be seen from this figure that at an x/L of .55 the bow shock intersects the trace of the wing leading edge in the $\Phi = 66°$ meridian ($\Phi = 0°$ is the windward plane). Downstream of this point the wing extends beyond the bow shock and the points of intersection of it on the upper and lower surfaces of the wing can easily be found. The trace of the bow shock on the wing will most definitely be a region of high heat transfer and one important to the thermal protection system design. It is believed that inclusion of the wing in the calculation will not significantly affect the intersection location. However, a more accurate representation of the fuselage at least near the nose could have a slight effect on this intersection location.

CROSS SECTIONAL SHOCK SHAPES FOR MSC 040 A FUSELAGE ONLY

M = 7.4 α = 15.3°

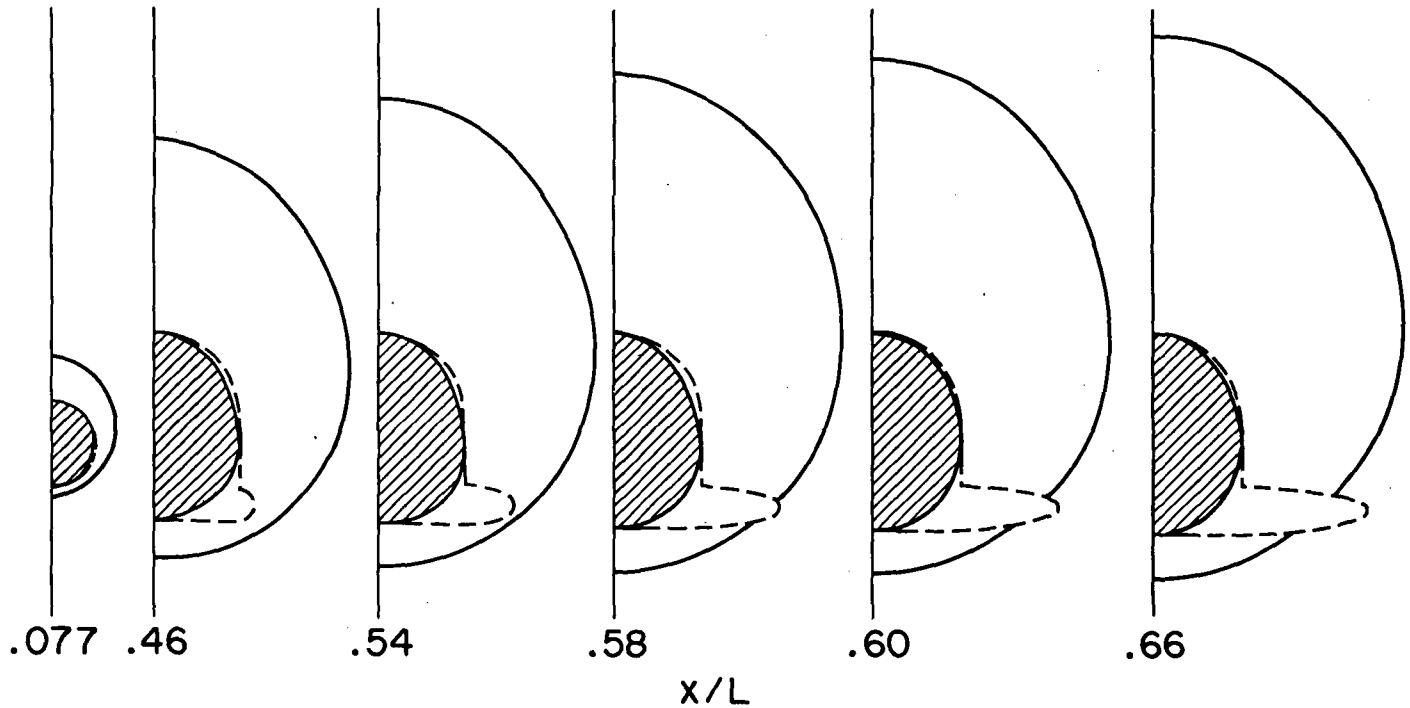

Figure 12

CONCLUDING REMARKS

(Figure 13)

We have presented some typical results obtained with two different computer codes currently in use at NASA-ARC for multidimensional supersonic flow fields. The relative merits of these methods are discussed in greater detail in another paper[4] which showed good agreement between results of the two methods. The shock capturing technique (SCT) is inherently more efficient than the characteristics code (MOC), being about four times faster on a point by point basis. The SCT code usually requires more mesh points than the MOC code when differencing across the bow shock. However, an advantage of using a large number of mesh points to describe the shock layer is that such things as the canopy shock, recompression shock and entropy layer can be accurately predicted. The use of a shock fitting procedure for the main bow shock is an obvious improvement, and work is in progress to develop such a code. This code would still allow the capturing of secondary shocks that form behind the bow shock. Considering its computational efficiency and ease in treating complex shock interaction, the SCT code may have an advantage over the present MOC program.

This paper may be considered a progress report on the efforts at Ames Research Center to develop a computational capability which can contribute, in a significant and timely way, to the design of the Space Shuttle vehicle. Some valuable work has been performed, but much remains to be done. For example, there is a need to include reaction chemistry in the calculations, so that the concentration of atomic species, which may control heat-shield performance, can be estimated. In addition the coupling of the inviscid and boundary-layer programs must be made more automatic. These are tasks that can be accomplished with the present methods and work is progressing in this direction.

SUMMARY

METHOD	ACCOMPLISHMENTS	PROBLEMS AND FUTURE EFFORT
SCT	COMPLEX SHUTTLE SHAPES SECONDARY SHOCKS INTERSECTING SHOCKS	WING LEADING EDGE EQUILIBRIUM GAS REACTING GAS
MOC	COMPLEX SHUTTLE SHAPES EQUILIBRIUM GAS DATA FOR BOUNDARY LAYER ANALYSIS	WING LEADING EDGE REACTING GAS SECONDARY SHOCKS

Figure 13

REFERENCES

1. Rakich, J. V.: Method of Characteristics for Steady Three-Dimensional Supersonic Flow With Application to Inclined Bodies of Revolution. TN D-5341, 1969, NASA.
2. Kutler, P., and Lomax, H.: Shock-Capturing, Finite-Difference Approach to Supersonic Flows. To be published in J. of Spacecraft and Rockets, Nov. or Dec., 1971.
3. Lomax, Harvard, and Inouye, Mamoru: Numerical Analysis of Flow Properties About Blunt Bodies Moving at Supersonic Speeds in an Equilibrium Gas. NASA TR R-204, 1964.
4. Rakich, John V., and Kutler, Paul: Comparison of Characteristics and Shock Capturing Methods With Application to the Space Shuttle Vehicle. Paper presented at the AIAA 10th Aerospace Sciences Meeting, San Diego, January 17-19, 1972.
5. Cleary, J. W.: Hypersonic Shock Wave Phenomena of a Delta-Wing Space Shuttle Orbiter. NASA TM X62,076.
6. Marvin, Joseph G. and Sheaffer, Yvonne S.: A Method for Solving the Nonsimilar Laminar Boundary-Layer Equations Including Foreign Gas Injection. NASA TN D-5516, 1969.
7. Lockman, William K., and DeRose, Charles E.: Aerodynamic Heating of a Space Shuttle Delta Wing Orbiter. TM X62,057, Aug. 1971.
8. Hamilton, H.H., and DeJarnette, F.R.: Inviscid Surface Streamline Program For Use In Predicting Shuttle Heating Rates. Space Shuttle Aerothermodynamics Technology Conference, Ames Research Center, Dec. 15-16, 1971.